

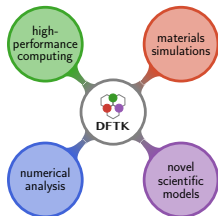
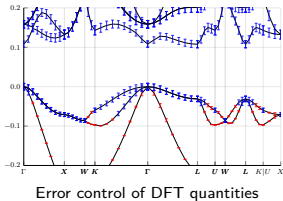
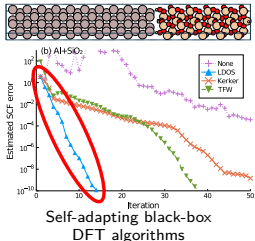
Black-box algorithms and robust error control for density-functional theory

Michael F. Herbst

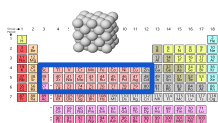
Applied and Computational Mathematics, RWTH Aachen University

26 April 2022

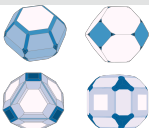
Slides: <https://michael-herbst.com/slides/epfl22>



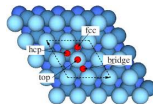
Task: Develop a new metallic catalyst for a surface reaction¹



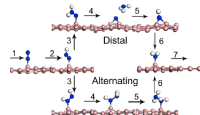
Host metal + dopant
 $\simeq 30 \times 30 = 900$



Host surface
 $\simeq 3 - 5$



Dopant adsorption site
 $\simeq 30$



Reaction intermediates
 $\simeq 10$

- Combinatorial design space: $\simeq 10^5 - 10^6$ possibilities
- Systematic experiments: Time and cost intensive
- ⇒ Computational screening to complement and accelerate
 - Harvest curated data bases
 - Data-driven methods and statistical learning
- ⇒ Regular need of millions of first-principle calculations
- Growing list of tools to manage workflows and curate data



¹ ACED project: <https://www.cmu.edu/aced/index.html>

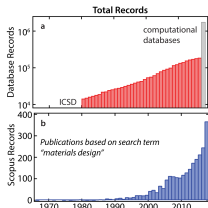
Status of high-throughput screening

- Exponentially growing impact
- Broad span of successful discoveries:^a
 - Semiconductors^b
 - Lithium-ion-based batteries^c
 - Magnetic compounds^d
 - 2D materials: Batteries^e, electronics^f

⇒ Crucial tool to tackle 21st century challenges

⇒ Standard method: Density-functional theory (DFT)

- Favourable cost / accuracy balance



^aK. Alberi *et. al.* J. Phys. D, **52**, 013001 (2019).

^bS. Luo *et. al.* WIREs Comput. Mol. Sci. **11**, e1489 (2021).

^cL. Kahle *et. al.* Energy & Environ. Science, **13**, 928 (2020).

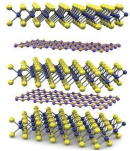
^dS. Jiang *et. al.* J. Alloys Comp. **867**, 158854 (2021).

^eA. Babak *et. al.* ACS Nano, **9**, 9507 (2015).

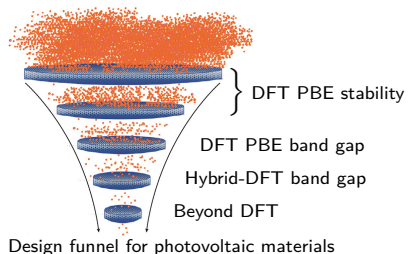
^fC. Klinkert *et. al.* ACS Nano, **14**, 8605 (2020).

<https://www.edfenergy.com/electric-cars/batteries>;

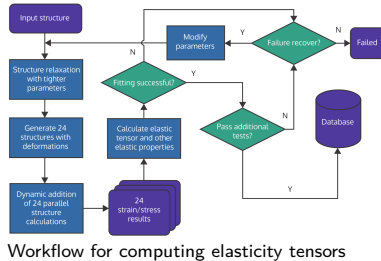
J. Evans *Beyond graphene Chemistry World* (2014).



Sketch of high-throughput workflows



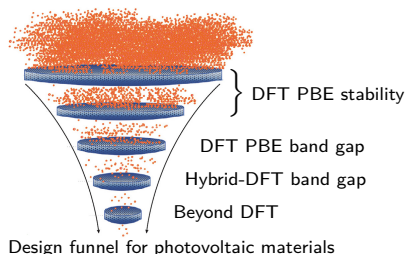
Design funnel for photovoltaic materials



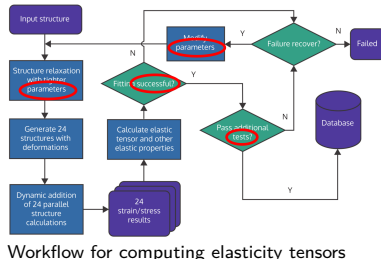
Workflow for computing elasticity tensors

- Many parameters to choose (algorithms, tolerances, models)
 - Elaborate heuristics: **Failure rate $\simeq 1\%$**
 - Still: **Thousands** of failed calculations
 - ⇒ Wasted resources & increased human attention (limits throughput)
- Carbon footprint? More complex design spaces?
- **Goal: Self-adapting black-box DFT algorithms**
 - Parameter-free, automatically adapt to simulated system
 - Transform **empirical wisdom** to built-in **convergence guarantees**

Sketch of high-throughput workflows



Design funnel for photovoltaic materials



Workflow for computing elasticity tensors

- Many parameters to choose (algorithms, tolerances, models)
 - Elaborate heuristics: **Failure rate $\simeq 1\%$**
 - Still: **Thousands** of failed calculations
⇒ Wasted resources & increased human attention (limits throughput)
- Carbon footprint? More complex design spaces?
- **Goal: Self-adapting black-box DFT algorithms**
 - Parameter-free, automatically adapt to simulated system
 - Transform **empirical wisdom** to built-in **convergence guarantees**

Broader vision: Robust & error-controlled simulations

- Error control = **Track simulation uncertainties:**
 - Self-adapting simulations with mathematical guarantees
 - Integrate with error propagation efforts for surrogates¹
 - ⇒ Byproducts: Data quality control, accelerated design²
 - Error control = **Learn missing physics:**
 - Data-enhanced models, active learning
 - Integration with experiment (autonomous discovery)
 - ⇒ Exploit high-fidelity experimental, beyond-DFT data
 - Error control = **Leverage inexactness:**
 - Error balancing: Optimal adaptive parameter selection
 - Randomised methods, selective precision (16-bit, FPGA)
 - Multi-fidelity approaches (reduced basis, surrogates)
- ⇒ Understand **where and how to spend efforts best**

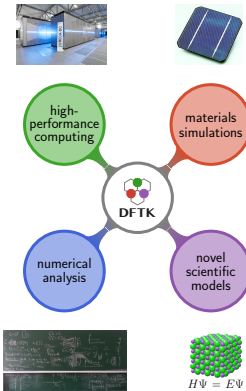
¹F. Musil, A. Grisafi et. al. J. Chem. Theo. Comput. **15**, 2 (2019).

²G. Houchins and V. Viswanathan MRS Bulletin **44**, 204 (2019).

Opportunities for mathematical research

- **Gap:** Mathematical understanding \Leftrightarrow simulation practice
- Broad range of concerned fields:
 - Optimisation, numerical linear algebra, analysis of PDEs, uncertainty quantification, model order reduction, ...
- Application domain: **Source for research problems**
 - Large-scale eigenvalue problems
(L. Lin, Y. Saad, C. Yang, ...)
 - Acceleration, fixed-point methods
(T. Kelly, A. Miedlar, Y. Saad, R. Schneider, H. vd. Vorst, H. Walker, ...)
 - Non-linear PDEs
(Z. Bai, E. Cancès, G. Friesecke, M. Lewin, I. Sigal, ...)
- Application domain: **Source for new methods**
 - Davidson diagonalisation (H. vd. Vorst, ...)
 - Thorough exploration of Anderson-type acceleration (see above)
- **17 minisymposia** at SIAM in 2021/22 (-CSE, -LA, -MS, -PP, -UQ)
with contributions related to **electronic-structure theory**

Opportunities for mathematical research (2)



- Role of mathematics: **Abstract and formalise**
 - Simplify and unify approaches (three methods are one)
 - New point of view \Rightarrow **New types of methods**
 - \Rightarrow Examples: SCF methods^{1,2}, acceleration^{3–5}
- Understand structure: **Shorter & simpler implementation**
- Rapid integration of **advances in computer science**
- \Rightarrow Boost in productivity
- **DFTK**: Lower barriers for **cross-disciplinary research**:
 - Allows restriction to **relevant model problems**,
 - *and scale-up* to application regime (1000 electrons)
 - **Sizeable feature set in 7000 lines of code**
 - MPI, self-adapting methods, algorithmic differentiation
 - **Integrated in multi-scale pipeline** (potential fitting, molecular dynamics)

¹A. Edelman, T. Arias *et. al.* J. Mat. Anal. Appl. **20**, 303 (1998).

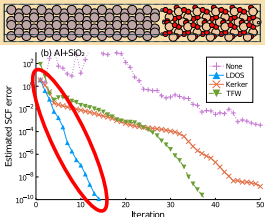
²E. Cancès, C. Le Bris *et. al.* Math. Model. Numer. Anal. **34**, 749 (2000).

³H. Fang Y. Saad Num. Lin. Alg. Appl. **16**, 197 (2009).

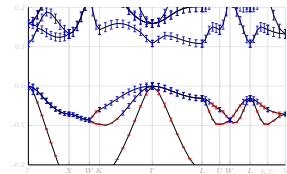
⁴H. Walker, P. Ni J. Num. Anal. **49**, 1715 (2011).

⁵M. Chupin, M. Dupuy *et. al.* Math. Model. Numer. Anal. **55** 2785 (2021).

Black-box algorithms and robust error control for DFT



Self-adapting black-box
DFT algorithms



- Density-functional theory
- Local density of states preconditioner
- Adaptive damping
- Errors in DFT
- Model sensitivities by algorithmic differentiation
- *A posteriori* error bounds for band structures



Density-functional theory (insulators)

- Goal: Understand electronic structures
 - Many-body quantum mechanics (Schrödinger equation)
- DFT approximation: Effective single-particle model

$$\left\{ \begin{array}{l} \forall i \in 1 \dots N : \left(-\frac{1}{2} \Delta + V(\rho_\Phi) \right) \psi_i = \varepsilon_i \psi_i, \\ V(\rho) = V_{\text{nuc}} + v_C \rho + V_{\text{xc}}(\rho), \\ \rho_\Phi = \sum_{i=1}^N |\psi_i|^2, \\ \Phi = (\psi_1, \dots, \psi_N) \in \left(L^2(\mathbb{R}^3, \mathbb{C}) \right)^N \text{ orthogonal} \end{array} \right.$$

nuclear attraction V_{nuc} , exchange-correlation V_{xc} , Hartree potential $-\Delta(v_C \rho) = 4\pi\rho$

⇒ Self-consistent field (SCF) problem: $V(\rho(V)) = V$ with

$$\rho(V) = \text{diag} \left[\mathbb{1}_{(-\infty, \varepsilon_F]} \left(-\frac{1}{2} \Delta + V \right) \right] \quad \text{and } \varepsilon_F \text{ s. t. } \int \rho(V) = N$$

- Hits plenty of “non-“s: Non-convex, non-linear, non-local, non-smooth

Self-consistent field problem

- Potential-mixing **SCF procedure** (preconditioner P , damping α)

$$V_{n+1} = V_n + \alpha P^{-1} [V(\rho(V_n)) - V_n]$$

- In practice: Combined with **acceleration** (e.g. Anderson)

- Dropped to simplify analysis
- Re-introduced for numerical experiments

- Near a fixed-point the error goes as

$$e_{n+1} \simeq [1 - \alpha P^{-1} \varepsilon] e_n$$

with dielectric matrix $\varepsilon = (1 - K\chi_0)$, $K(\rho) = V'(\rho)$, $\chi_0(V) = \rho'(V)$

- Convergence iff $-1 < [1 - \alpha P^{-1} \varepsilon] < 1$

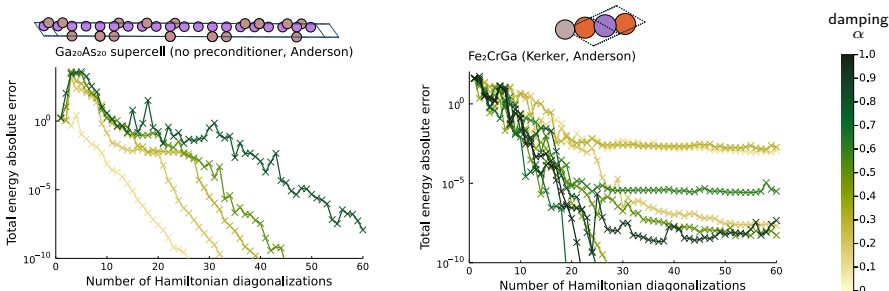
- Dielectric matrix ε : **Depends on physics** (conduction, screening)
- Second-order conditions: $\varepsilon \geq 0$ (near fixed point)

⇒ Need $P^{-1} \simeq \varepsilon^{-1}$ (**matching preconditioner**) or small α

Drawback of established approaches

1. Preconditioner P is system-dependent and *chosen a priori*
 - Standard preconditioners: Derived from **bulk materials**
 - Misses important applications (e.g. **inhomogeneous systems**)
 - E.g. clusters, passivated surfaces, heterogeneous catalysis, . . .
 2. If no good preconditioner P known: **Trial and error**
 - Employ standard heuristics: E.g. **decrease damping α**
 - But: Can fail for interesting cases (**the tough 1%** ?)
- ⇒ Wasted computational resources
- ⇒ **Goal:** Black-box and **self-adapting** P and α

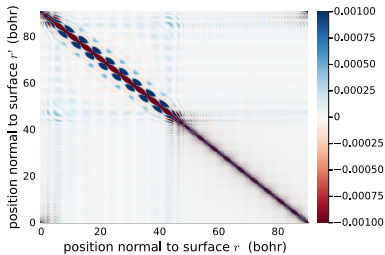
Illustration: Guessing a suitable damping α can be hard



- Inefficient standard damping (0.6 – 0.8)
- Surprisingly small damping for smooth convergence
- Heusler alloy: Design space of interest
- High-throughput study at EPFL: Convergence difficulties
- Irregular behaviour: α versus convergence
- Heuristics breaks: Larger damping is better

Black-box P : Local density of states (LDOS) mixing¹

- Bulk preconditioning models approximate inverse $P^{-1} \simeq \varepsilon^{-1}$
- Use $\varepsilon = (1 - K\chi_0)$ with $K(\rho) = V'(\rho)$, $\chi_0(V) = \rho'(V)$
- $\chi_0(r, r')$ unit-cell internal fluctuations, diagonal dominant:



- Tackle **charge sloshing**: Consider large-scale variations of χ_0 :

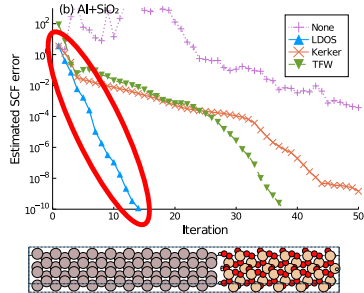
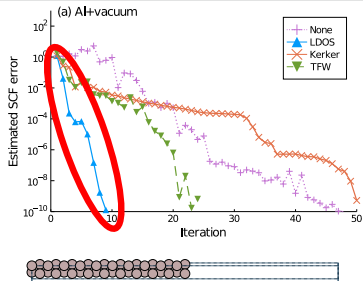
$$\chi_0(r, r') \simeq -\text{LDOS}(r)\delta(r, r') \quad (\text{homogenised } \chi_0)$$

- Apply preconditioner **iteratively**:

$$P^{-1}V_n = [1 - K\widetilde{\chi}_0)]^{-1}V_n, \quad \widetilde{\chi}_0(r, r') = -\text{LDOS}(r)\delta(r, r')$$

¹MFH, A. Levitt. J. Phys. Condens. Matter **33**, 085503 (2021).

LDOS preconditioning (examples)¹



- Inhomogeneous material: Aluminium metal + Insulator
- TFW: local Thomas-Fermi-von Weizsäcker mixing²
(Ad hoc modification of metallic screening model)
- LDOS automatically interpolates between Kerker mixing
(suitable for metals) and no mixing (suitable for insulators)
 - ⇒ Based on mathematical understanding of screening
 - ⇒ Parameter-free and black-box

¹MFH, A. Levitt. J. Phys. Condens. Matter **33**, 085503 (2021).

²D. Raczkowski, A. Canning, L. W. Wang, Phys. Rev. B **64**, 121101 (2001).

Black-box α : Adaptive damping¹

- Which damping α in potential mixing?
 - $V_n \rightarrow$ Find search direction δV_n (preconditioning, Anderson, ...)
 - $V_{n+1} = V_n + \alpha \delta V_n$
- DFT is an energy minimisation problem $\min_V \mathcal{E}(V)$
- **Theorem (Herbst, Levitt 2022):¹**
 - Guaranteed convergence if α small enough
- **Ingredient 1:** Backtracking line search:
 - Start from trial damping $\tilde{\alpha}$ and set $\alpha = \tilde{\alpha}$
 - Accept good steps (energy or SCF residual decreases)
 - Otherwise: Shrink α and try again
- But: Expensive step of an SCF is $\rho(V)$ (involves H diagonalisation)
 - Needed for evaluating $\mathcal{E}(V_n + \alpha \delta V_n)$
 - ⇒ Cost of line search step \simeq cost of standard SCF step

¹MFH, A. Levitt. J. Comput. Phys. **459**, 111127 (2022).

Adaptive damping (2)

- **Ingredient 2:** Shrink α by approx. quadratic model for $\mathcal{E}(V_n + \alpha \delta V_n)$

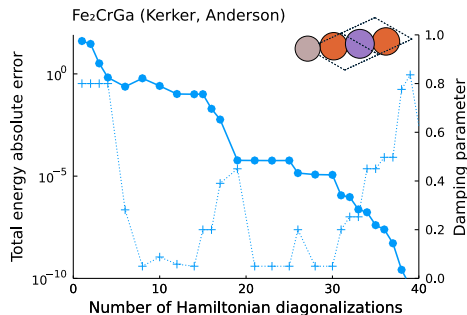
- Key approximation:

$$\alpha \chi_0(V_n) \delta V_n = \rho(V_n + \alpha \delta V_n) - \rho(V_n) + O(\alpha^2 \|\delta V_n\|^2)$$

- (a) Avoids costly χ_0 application (involves solving linear system)
- (b) If accepted: $\rho(V_n + \alpha \delta V_n) = \rho(V_{n+1})$
⇒ Reuse ρ in next SCF step

- No overhead if line search immediately successful

⇒ Use quadratic model also to adjust trial damping $\tilde{\alpha}$



Selected results¹: Diagonalisations to convergence

System		fixed damping α										adaptive damping
		0.1	0.2	0.3	0.4	0.5	0.6	0.7	0.8	0.9	1.0	
simple	Al ₄₀ slab	19	15	14	12	11	12	12	12	12	12	12
transition metal	Fe ₂ CrGa	x	x	x	27	x	x	19	25	x	22	39
	Fe ₂ MnAl	x	48	x	x	x	20	21	17	16	15	34
	FeNiF ₆	x	x	x	x	x	x	x	23	22	21	24
	Fe ₂₈ W ₈ bilayer	32	34	37	34	38	43	41	48	x	x	37

x: Energy not converged to 10^{-10} after 100 diagonalisations

- Simple systems: Adaptive has almost **no additional cost**
- Transition-metal systems with challenging setup (Details: paper)
 - Successful/best α scattered \Rightarrow **Manual selection challenging**
 - Artefact of Anderson acceleration (not covered by Theorem)
 - Adaptive** has overhead, but **avoids trial and error**
 \Rightarrow Mathematically motivated **safeguard mechanism**
- \Rightarrow Limitations in mathematical understanding of acceleration

¹MFH, A. Levitt. J. Comput. Phys. **459**, 111127 (2022).

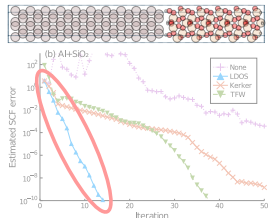
Summary and future work

- Black-box strategies for damping¹ α & preconditioning² P
 - Build on combining mathematical and physical insight
 - Integrate with standard SCF techniques (e.g. acceleration)
 - Readily available in  DFTK
- ⇒ Safeguard mechanism: Increase robustness for hard cases
- Lack of mathematical understanding of acceleration schemes
 - E.g. sensitivity to numerical noise (incomplete diagonalisation)
- Extensions to LDOS mixing:
 - Description of polarisation (semiconductors)
 - Localised states (transition metal alloys)

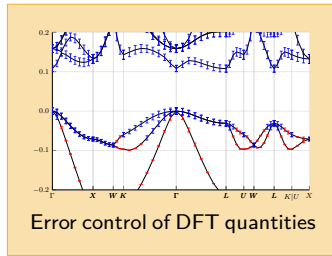
¹MFH, A. Levitt. J. Comput. Phys. **459**, 111127 (2022).

²MFH, A. Levitt. J. Phys. Condens. Matter **33**, 085503 (2021).

Black-box algorithms and robust error control for DFT



Self-adapting black-box
DFT algorithms



- Density-functional theory
- Local density of states preconditioner
- Adaptive damping
- Errors in DFT
- Model sensitivities by algorithmic differentiation
- *A posteriori* error bounds for band structures



Error sources in DFT simulations

- Model error: Selection of DFT model
- Computational approach:
 - Discretisation error: Basis size, k -point mesh
 - Algorithm error: Convergence thresholds (SCF, eigensolver)
 - Floating-point error: Floating-point arithmetic
- Additionally: Programming error, hardware error (not discussed further)
- Error control: Link parameter selection \leftrightarrow simulation error
 - Enables error balancing
 - Optimised automatic parameter selection

⇒ Robust, parameter-free & efficient simulations

Status of error control in DFT

- Statistical techniques ⇒ **Model error**
 - Ensemble-mediated (BEEF)¹
 - Representative comparison (Δ -test)²
 - **This talk:** (A) Model sensitivities by algorithmic differentiation
⇒ Outlook: Efficient inference of DFT model uncertainties
- Numerical analysis ⇒ **Discretisation error**
 - k -point sampling³, eigenvalue clusters⁴
 - Perturbation-based bounds for Gross-Pitaevskii⁵ and DFT⁶
 - Application & implementation: Restricted setting
 - **This talk:** (B) Guaranteed bounds for band structures in a pseudopotential model

¹V. Petzold, T. Bligaard *et. al.* Top. in Catal., **55**, 402 (2012).

²K. Lejaeghere, G. Bihlmayer *et. al.* Science, **351**, aad3000 (2016).

³E. Cancès, V. Ehrlacher *et. al.* Numer. Math. **144**, 479 (2020).

⁴E. Cancès, G. Dusson *et. al.* Math. Comp. **89**, 2563 (2020).

⁵E. Cancès, G. Dusson *et. al.* Comp. Rend. Math. **352**, 941 (2014).

⁶E. Cancès, G. Dusson *et. al.* arxiv 2111.01470v1.

(A): Routine computation of DFT model sensitivities

- Efficient inference strategies for uncertainty quantification:
 - Requires sensitivities wrt. DFT model
 - ⇒ Unusual, higher-order derivatives
- Combinatorial explosion:
 - “One PhD student per derivative” paradigm not feasible
 - ⇒ Use algorithmic differentiation (\approx automatic derivatives)
- Illustration: Consider DFT Hamiltonian $H_{a\theta}$
 - a : Lattice constant
 - θ : DFT exchange-correlation parameters
- Self-consistent field yields fixed-point density ρ_{SCF}

$$0 = \text{diag} \left[\mathbb{1}_{(-\infty, \varepsilon_F]}(H_{a\theta}(\rho_{\text{SCF}})) \right] - \rho_{\text{SCF}}$$

- Defines implicit function $\rho_{\text{SCF}}(a, \theta)$

Computing sensitivities

- Consider **model sensitivity** of stress $S(a, \theta) = \frac{\partial \mathcal{E}(\rho_{\text{SCF}}(a, \theta))}{\partial a}$:

$$\frac{dS}{d\theta} = \frac{\partial S}{\partial \rho_{\text{SCF}}} \frac{\partial \rho_{\text{SCF}}}{\partial \theta} \quad (1)$$

- Computed by **implicit differentiation** (response theory):

$$\frac{\partial \rho_{\text{SCF}}}{\partial \theta} = [1 - \chi_0 K]^{-1} \chi_0 \frac{\partial H_{a\theta}}{\partial \theta}$$

- Parameters appear in innermost layer (model definition)
 - Each DFT model: Different derivatives $\frac{\partial H_{a\theta}}{\partial \theta}$ (can be horrible)
 - Each quantity of interest: Different sensitivity expression (1)
⇒ Combinatorial explosion
- Opportunity of algorithmic differentiation (AD):
 - Generic framework for DFT derivatives / response properties
 - Saves manual coding: Request gradient (1), AD delivers
⇒ New properties/derivatives by non-DFT experts!

Preview: Algorithmic differentiation in DFT practice

- **Optimal lattice constant:** Optimal size of the unit cell:

$$a_* = \arg \min_a \mathcal{E}[\rho_{\text{SCF}}(a, \theta)]$$

```
function dft_energy(a, θ)
    model = Model(a, PbeExchange(θ), ...)
    scf(model).energies.total
end
optimise_lattice(θ) = optimise(a → dft_energy(a, θ))
```

- How sensitive is a_* for a system? \Rightarrow Need $\frac{da_*}{d\theta}$
- Annoyances for derivation and implementation:
 - Nested iterative methods (eigensolver, SCF, lattice optimisation)
 - Unusual second-order derivatives (e.g. $\frac{\partial S}{\partial \theta} = \frac{\partial^2 \mathcal{E}}{\partial \theta \partial a}$)
 - Will it still work for future DFT models?
(with completely different kinds of parameters θ)
- With  DFTK: User needs to add one line of code

Preview: Algorithmic differentiation in DFT practice

- Optimal lattice constant: Optimal size of the unit cell:

$$a_* = \arg \min_a \mathcal{E}[\rho_{\text{SCF}}(a, \theta)]$$

```
function dft_energy(a, θ)
    model = Model(a, PbeExchange(θ), ...)
    scf(model).energies.total
end
optimise_lattice(θ) = optimise(a → dft_energy(a, θ))

sensitivities =
    ForwardDiff.gradient(optimise_lattice, [κ, β])
```

- How sensitive is a_* for a system? \Rightarrow Need $\frac{da_*}{d\theta}$
- Annoyances for derivation and implementation:
 - Nested iterative methods (eigensolver, SCF, lattice optimisation)
 - Unusual second-order derivatives (e.g. $\frac{\partial S}{\partial \theta} = \frac{\partial^2 \mathcal{E}}{\partial \theta \partial a}$)
 - Will it still work for future DFT models?
(with completely different kinds of parameters θ)
- With  DFTK: User needs to add one line of code

Preview: Lattice constant sensitivities of silicon

```
function dft_energy(a, θ)
    model = Model(a, PbeExchange(θ), ...)
    scf(model).energies.total
end
optimise_lattice(θ) = optimise(a -> dft_energy(a, θ))

sensitivities =
    ForwardDiff.gradient(optimise_lattice, [κ, β])
```

(Å)	a_*	κ	$\frac{da_*}{d\kappa}$	β	$\frac{da_*}{d\beta}$
expmnt.	5.421				
PBEsol	5.449	0.804	0.713	0.0375	0.0058
PBE	5.461	0.804	0.550	0.0667	0.0194
APBE	5.465	0.804	0.482	0.0790	0.0269
PBEmol	5.467	0.804	0.456	0.0838	0.0301
XPBE	5.466	0.920	0.603	0.0706	0.0184
rev-PBE	5.467	1.245	0.744	0.0667	0.0099

Model sensitivities for the silicon lattice constant

- Generic framework building on:

- Flexible  DFTK architecture (floating-point agnostic)
-  Julia tools for algorithmic differentiation
- Extra work: Generic response implementation in  DFTK

- Fully flexible in DFT model or targeted quantity:

- Only XC energy expression & SCF postprocessing code needed

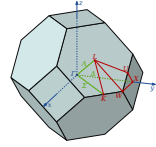
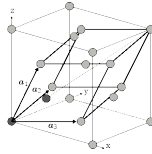
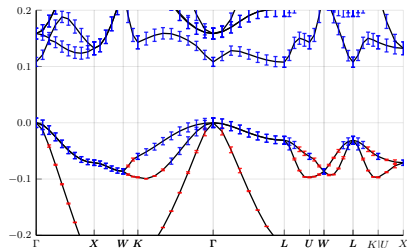
- Ongoing: Adjoint-mode AD implementation:

- All parameter sensitivities by a single response problem

⇒ Routine computation of model sensitivities

⇒ Machine-learned solid-state XC models (where θ high-dimensional)

(B): Bounds on band structures (eigenvalues of H)



- Band structure: Plot of $k \in \text{BZ}$ versus eigenvalues of

$$H_k = \frac{1}{2}(-i\nabla + k)^2 + V_{\text{nuc}} + \cancel{v_C\rho} + \cancel{V_{XC}(\rho)} \quad (\text{linear \& non-local})$$

- First consideration of a pseudopotential model
 - Simple & fully guaranteed bounds for an application setting
- Today: Discretisation error in plane-wave basis

$$X = \text{span} \left\{ e_G \mid \frac{1}{2} |G + k|^2 \leq E_{\text{cut}} \right\} \quad \text{with } e_G(r) = \frac{1}{\sqrt{|\Omega|}} e^{iG \cdot r}$$

¹MFH, A. Levitt, E. Cancès. Faraday Discuss. 223, 227 (2020).

Setting: Pseudopotential Hamiltonians¹

- $\langle \cdot | \cdot \rangle$: L^2_{per} inner product; $\| \cdot \|$: L^2_{per} norm, $\| \cdot \|_{\text{op}}$: Operator norm on $\mathcal{L}(L^2_{\text{per}})$
- Plane-wave basis and pseudopotential in Kleinman-Bylander form:

$$\begin{aligned}\langle e_G | H e_{G'} \rangle = & \frac{1}{2} |G + k|^2 \delta_{GG'} + \frac{\widehat{v}_{\text{loc}}(G - G')}{|\Omega|} \\ & + \sum_{Lij} d_{Lij} \widehat{p_{Li}}(k + G) \overline{\widehat{p_{Lj}}(k + G')}\end{aligned}$$

with $\widehat{p_{Li}}(q) = Y_L(q/|q|)R_i(|q|)$, Y_L spherical harmonics.

⇒ Non-local, i.e. not multiplicative V

- Fourier coefficients $\widehat{v}_{\text{loc}}(G)$ and $R_i(|k + G|)$ decay quantitatively for $|G| > q_{\min}$ with q_{\min} small. (Potential regularity)
- Satisfied e.g. for Goedecker-type pseudopotentials

¹MFH, A. Levitt, E. Cancès. Faraday Discuss. 223, 227 (2020).

A posteriori error estimation for eigenvalues

- Color coding: Unknown quantities, computable quantities
 - Exact solution: $Hu = \varepsilon u$
 - Discretised solution: $\tilde{H}\tilde{u} = \tilde{\varepsilon}\tilde{u}$
 - Goal: Error $|\tilde{\varepsilon} - \varepsilon|$... but ε unknown
- ⇒ Invoke a residual-error relationship. We keep it simple:

$$|\tilde{\varepsilon} - \varepsilon| \leq \frac{\|r\|^2}{\delta} \quad (\text{Kato-Temple}), \quad \text{gap } \delta$$

- where r is the eigenpair residual $r = H\tilde{u} - \tilde{\varepsilon}\tilde{u}$
 - Exact H unknown $\Rightarrow \|r\|$ still unknown
 - But: Can get computable upper bound $\|r\| \leq f(\tilde{\varepsilon}, \tilde{u}, \tilde{H})$
- ⇒ Overall strategy:
- Upper bound on $\|r\|$
 - Lower bound on gap δ

L^2 -residual upper bound

- Define the larger basis

$$Y = \text{span} \left\{ e_G \mid \frac{1}{2} |G + k|^2 \leq E_{\text{cut}}^{(2)} \right\}$$

with $E_{\text{cut}}^{(2)} \geq \frac{1}{2} q_{\min}^2 > E_{\text{cut}}$. Assume V can be computed on Y .

- Denote P_Y as projector into Y basis and split:

$$\|r\| = \|P_Y r\| + \|P_{Y^\perp} r\| = \|P_Y H \tilde{u} - \tilde{\varepsilon} \tilde{u}\| + \|P_{Y^\perp} V \tilde{u}\|$$

Note: $\tilde{u} \in X \subset Y$, kinetic energy is diagonal.

- First term computable, second term is

$$\|P_{Y^\perp} V \tilde{u}\|^2 = \sum_{G \in Y^\perp} \left| \sum_{G' \in X} \langle e_G | V e_{G'} \rangle \tilde{u}(G') \right|^2$$

- By construction: $\hat{v}_{\text{loc}}(G)$ and $p_{Li}(k + G)$ decay outside Y

\Rightarrow Elements $\langle e_G | V e_{G'} \rangle$ coupling X and Y^\perp are small

$\Rightarrow \|P_{Y^\perp} V \tilde{u}\|$ has computable upper bound.

- Use Fourier kernel / pseudopotential projector structure + tail sum bound

Obtaining a gap lower bound

- Seek $\mu \leq \varepsilon_{n+1}$, s.t. $\mu - \tilde{\varepsilon}_n \leq \varepsilon_{n+1} - \varepsilon_n = \delta$
- Partition H into part in X and outside:

$$H = \begin{pmatrix} H_{XX} & V_{XX^\perp} \\ V_{X^\perp X} & H_{X^\perp X^\perp} \end{pmatrix} \quad (\text{kin. op. diagonal})$$

Theorem (Herbst, Levitt, Cancès 2020)

Let H be of the specified pseudopotential form. For a μ with $\tilde{\varepsilon}_n \leq \mu \leq \tilde{\varepsilon}_{n+1}$ it holds $\varepsilon_n \leq \mu \leq \varepsilon_{n+1}$ provided that

$$\begin{aligned} \tilde{S}_\mu &= E_{\text{cut}} - \|V_{X^\perp X^\perp}\|_{\text{op}} - \mu + \tilde{B}_\mu \geq 0 \\ \tilde{B}_\mu &= - \left\| (V_{X^\perp \cap Y, X} U) (\Lambda - \mu)^{-1} (V_{X^\perp \cap Y, X} U)^\dagger \right\|_{\text{op}} \\ &\quad - 2 \left\| (V_{X^\perp \cap Y, X} U) (\Lambda - \mu)^{-1} \right\|_{\text{op}} \|V_{X, Y^\perp}\|_{\text{op}} \\ &\quad - \frac{\|V_{X, Y^\perp}\|_{\text{op}}^2}{\tilde{\varepsilon}_N - \mu}, \end{aligned}$$

where $H_{XX} = U \Lambda U^\dagger$, $N = \dim(X)$ and subscripts denote projections into X and Y or the respective orthogonal complements.

Proof eigenvalue lower bound

- Haynsworth inertia additivity formula:

$$\sigma_-(H - \mu) = \sigma_-(H_{XX} - \mu) + \sigma_-(S_\mu)$$

where the Schur complement

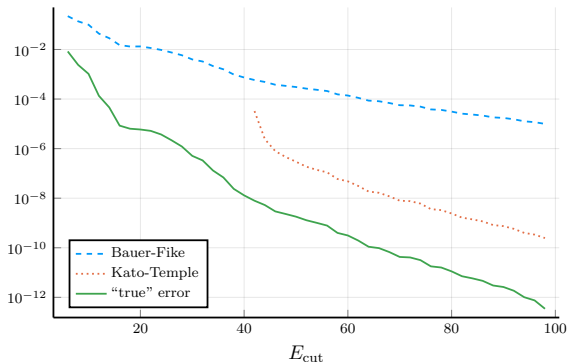
$$S_\mu = (H_{X^\perp X^\perp} - \mu) - V_{X^\perp X} (H_{XX} - \mu)^{-1} V_{XX^\perp}$$

- By construction: $\sigma_-(H_{XX} - \mu) = n$
- Therefore: $\sigma_-(S_\mu) = 0 \Leftrightarrow \sigma_-(H - \mu) = n \Leftrightarrow \mu \leq \varepsilon_{n+1}$
- We bound S_μ from below:

$$\begin{aligned} S_\mu &\geq E_{\text{cut}} - \|V_{X^\perp X^\perp}\|_{\text{op}} - \mu + B_\mu \\ B_\mu &= -\|V_{X^\perp X} U (\Lambda - \mu)^{-1} U^\dagger V_{XX^\perp}\|_{\text{op}} \\ &\geq -\left\| (V_{X^\perp \cap Y, X} U) (\Lambda - \mu)^{-1} (V_{X^\perp \cap Y, X} U)^\dagger \right\|_{\text{op}} \\ &\quad - 2 \left\| (V_{X^\perp \cap Y, X} U) (\Lambda - \mu)^{-1} \right\|_{\text{op}} \|V_{X, Y^\perp}\|_{\text{op}} \\ &\quad - \frac{\|V_{X, Y^\perp}\|_{\text{op}}^2}{\tilde{\varepsilon}_N - \mu} \end{aligned}$$

□

Numerical results for the eigenvalue discretisation error¹



- GTH Silicon, 1st eigenvalue, largest admissible μ
- Gap only found from $E_{\text{cut}} = 40$ (before no μ admissible)
- Improvements:
 - Better operator norm bounds
 - Integration with energy-norm-based approaches

¹MFH, A. Levitt, E. Cancès. Faraday Discuss. 223, 227 (2020).

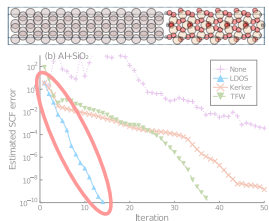
Summary and future work

- Two thrusts for routine error control in DFT simulations
 - Algorithmic differentiation for DFT sensitivities
 - First guaranteed error bounds for pseudopotential model¹
- Completing the DFT error picture:
 - Combination of analytical and statistical approaches
 - Better understanding of the floating-point error
 - ⇒ Automatic parameter selection & approximate computing
- Quantifying DFT model uncertainties:
 - Bayesian analysis of multi-model ensembles² (ongoing)
 - ⇒ Multi-fidelity methods

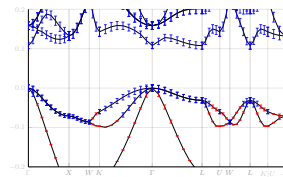
¹MFH, A. Levitt, E. Cancès. Faraday Discuss. **223**, 227 (2020).

²C. Tebaldi, R. Smith *in* The Oxford handbook of applied Bayesian analysis (2010)

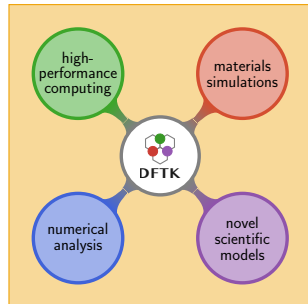
Black-box algorithms and robust error control for DFT



Self-adapting black-box
DFT algorithms



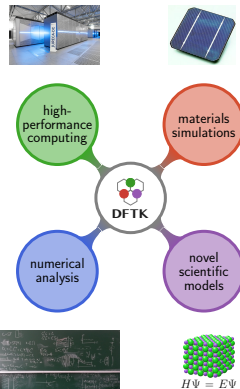
Error control of DFT quantities



- Density-functional theory
- Local density of states preconditioner
- Adaptive damping
- Errors in DFT
- Model sensitivities by algorithmic differentiation
- *A posteriori* error bounds for band structures

●  **DFTK overview**

Density-functional toolkit¹ — <https://dftk.org>



- **julia** code for plane-wave DFT, started in 2019
- Fully composable with **julia** ecosystem:
 - Arbitrary precision (32bit, >64bit, ...)
 - Algorithmic differentiation (AD)
- Key tool in all presented research:
 - Mathematical analysis (GPE, reduced models)
 - Scale-up to applications ($\simeq 1000$ electrons)
 - Features incl. meta-GGA, response, MPI parallelisation
 - Speed within factor 2–4 to established codes
- ⇒ Build to enable **multidisciplinary synergies**
- Low entrance barrier **across backgrounds**:
 - Only 7000 lines of code, open-source components
 - Avoids **two-language problem**: Just **julia**
- High-productivity research framework:
 - 10 weeks to submit *a posteriori* paper
 - GSoC student (10 weeks) for initial AD support



- Self-adapting black-box DFT methods^{a,b}
- Numerical analysis of DFT^c
- Practical error bounds^{d,e}
- Exploring algorithmic differentiation:
 - “Automatic response”: Phonons & higher-order properties
 - Full AD-able simulation pipeline: DFT, potentials, MD
- Uncertainty quantification all the way: DFT, potentials, MD
- Approximate computing on modern GPUs
- Outreach and teaching
 - Community building: **julia**-based first-principle ecosystem
 - Lecture: Mathematics of computational chemistry

Growing user base:



^aMFH, A. Levitt. J. Phys. Condens. Matter **33**, 085503 (2021).

^bMFH, A. Levitt. J. Comput. Phys. **459**, 111127 (2022).

^cE. Cancès, G. Kemlin et. al. J. Matrix Anal. Appl., **42**, 243 (2021).

^dMFH, A. Levitt, E. Cancès. Faraday Discuss. **223**, 227 (2020).

^eE. Cancès, G. Dusson et. al. arxiv 2111.01470v1.

Opportunities to learn more . . .



CECAM workshop (*with G. Csányi, G. Dusson, Y. Marzouk*):

“Error control in first-principles modelling”

- **20–24 June 2022** (hybrid & CECAM-HQ, Lausanne)

⇒ <https://www.cecam.org/workshop-details/1115>



DFTK school 2022 (*with E. Cancès, A. Levitt*):

“Numerical methods for DFT simulations”

- **29–31 August 2022** at Sorbonne Université, Paris
- Centred around DFTK and its multidisciplinary philosophy
- Grounds-up introduction of electronic structure theory, mathematical background, numerical methods, implementation
- Applications in method development & simulations

⇒ <https://school2022.dftk.org> Deadline: 30th April

Acknowledgements

<https://michael-herbst.com/slides/epfl22>

École des Ponts

Antoine Levitt

Eric Cancès

RWTH

Benjamin Stamm

Markus Towara

EPFL

Marnik Bercx

Nicola Marzari

MIT

Jeremiah DeGreeff

Katharine Fisher

Youssef Marzouk

Emmanuel Luján

TU Berlin

Niklas Schmitz

all DFTK contributors



Applied and
Computational
Mathematics

RWTHAACHEN
UNIVERSITY

Inria



École des Ponts
ParisTech



Summer of code



European Research Council
Established by the European Commission

julia

MIT

CESMIX

Questions?

<https://michael-herbst.com/slides/epfl22>

 [mfherbst](https://github.com/mfherbst)

 herbst@acom.rwth-aachen.de

 <https://michael-herbst.com/blog>

 **DFTK** <https://dftk.org>

<https://school2022.dftk.org>

 <https://www.cecam.org/workshop-details/1115>

 <https://michael-herbst.com/learn-julia>

Contents

- 4 LDOS preconditioner
- 5 Adaptive damping
- 6 Algorithmic differentiation
- 7 A posteriori



Applied and
Computational
Mathematics

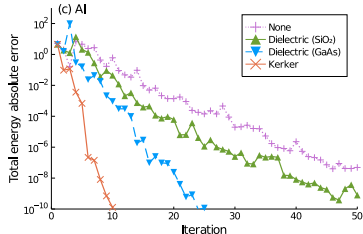
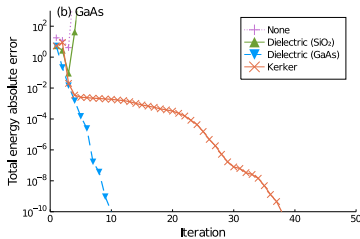
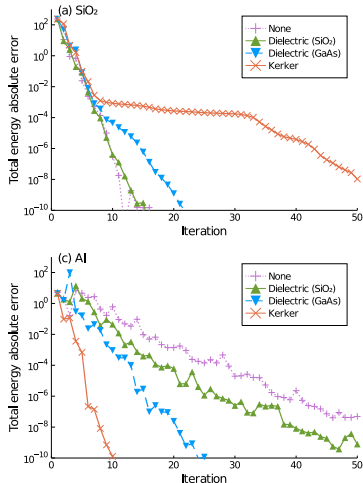
RWTH AACHEN
UNIVERSITY

SCF instabilities

$$e_{n+1} \simeq [1 - \alpha P^{-1} \varepsilon] e_n, \quad \varepsilon = 1 - (v_C + K_{\text{xc}}) \chi_0$$

- SCF instabilities increase condition number κ :
 - ε has small eigenvalues (e.g. symmetry breaking)
 - χ_0 has large eigenvalues (localised states)
 - Large charge-sloshing modes of v_C are uncompensated by χ_0 (metals)
- ⇒ Need infeasibly small α or good P
- Physics where a good mixing P is known:
 - Bulk insulators ($P = I$)
 - Bulk metals (Kerker mixing)
 - Bulk semiconductors (e.g. Resta's dielectric model)

Convergence results for bulk materials¹



- silica (SiO_2) insulator
- gallium arsenide (GaAs) semiconductor
- aluminium (Al) metal

¹M. F. Herbst, A. Levitt. J. Phys. Condens. Matter **33**, 085503 (2021).

Local density of states (LDOS) approximation for χ_0 ¹

- Adler-Wiser formula (with occupation function f):

$$\chi_0(\underline{r}, \underline{r}') = \sum_{n,m} \frac{f(\varepsilon_n) - f(\varepsilon_m)}{\varepsilon_n - \varepsilon_m} \psi_n(\underline{r}) \psi_m^*(\underline{r}) \psi_m(\underline{r}') \psi_n^*(\underline{r}')$$

- Large-scale variations from V_n to V_{n+1} :

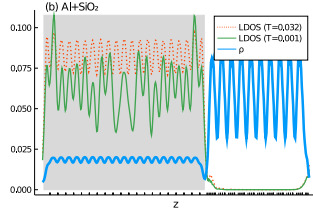
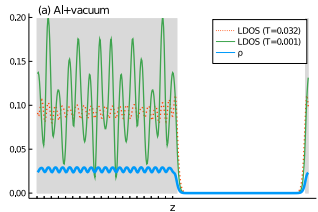
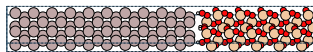
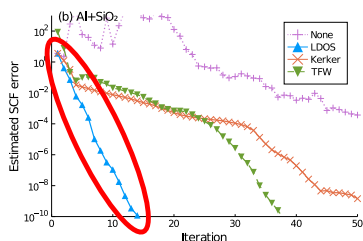
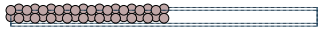
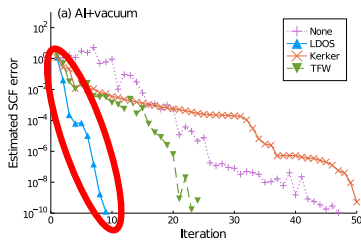
⇒ Assume $\underline{r} \mapsto \chi_0(\underline{r}, \underline{r}')$ more localised around \underline{r}' than $V_i(\underline{r}')$.

- “Row-sum mass lumping”:

$$\begin{aligned}\int \chi_0(\underline{r}, \underline{r}') V(\underline{r}') \mathrm{d}\underline{r}' &\simeq V(\underline{r}) \int \chi_0(\underline{r}, \underline{r}') \mathrm{d}\underline{r}' \\&= V(\underline{r}) \sum_{n,m} \frac{f(\varepsilon_n) - f(\varepsilon_m)}{\varepsilon_n - \varepsilon_m} \psi_n(\underline{r}) \psi_m^*(\underline{r}) \delta_{mn} \\&= V(\underline{r}) \sum_n f'(\varepsilon_n) |\psi_n(\underline{r})|^2 \\&= V(\underline{r}) \cdot \left(-\text{LDOS}(\underline{r}) \right)\end{aligned}$$

¹M. F. Herbst, A. Levitt. J. Phys. Condens. Matter **33**, 085503 (2021).

LDOS preconditioning (examples)¹



²D. Raczkowski, A. Canning, L. W. Wang, Phys. Rev. B. **64**, 121101 (2001).

¹MFH, A. Levitt. J. Phys. Condens. Matter **33**, 085503 (2021).

LDOS preconditioning results¹

	\mathcal{N}	None		Dielectric		Kerker		LDOS		LDOS+ Dielectric	
		it	κ	it	κ	it	κ	it	κ	it	κ
$\text{SiO}_2 + \text{vacuum}$	10	11	3.3	26	19.7	50	95.7	11	3.3	26	19.7
	20	12	3.4	30	24.4	n.c.	351.5	12	3.4	30	21.7
$\text{GaAs} + \text{vacuum}$	10	17	13.4	18	6.2	23	67.0	17	12.4	18	10.4
	20	20	15.5	22	12.9	n.c.	312.2	20	15.5	22	12.9
$\text{Al} + \text{vacuum}$	10	19	51.5	24	44.3	22	64.4	9	3.7	16	10.3
	20	47	170.8	49	168.5	n.c.	323.9	9	3.5	20	10.5
$\text{GaAs} + \text{SiO}_2^{\text{a}}$	10	45	13.7	19	8.9	34	52.4	45	13.4	19	8.8
	20	n.c.	18.2	20	10.2	n.c.	170.1	n.c.	18.2	20	10.2
$\text{Al} + \text{SiO}_2$	10	43	93.1	29	33.6	30	50.9	17	6.1	20	9.2
	20	n.c.	316.6	n.c.	118.4	n.c.	159.4	14	5.4	20	10.1
$\text{Al} + \text{GaAs}$	10	n.c.	144.0	24	22.4	16	9.0	15	7.2	11	3.5
	20	n.c.	485.0	40	59.0	26	28.8	26	21.4	13	5.0
$\text{Al} + \text{GaAs} + \text{SiO}_2$	10	n.c.	149.5	34	50.4	36	62.9	26	21.5	19	9.0

- Coloured: Condition number κ less than doubled on doubling system size

¹MFH, A. Levitt. J. Phys. Condens. Matter **33**, 085503 (2021).

Contents

- 4 LDOS preconditioner
- 5 Adaptive damping
- 6 Algorithmic differentiation
- 7 A posteriori



Applied and
Computational
Mathematics

RWTHAACHEN
UNIVERSITY

Constructing the model (1)

- Use Taylor ...

$$\begin{aligned}\mathcal{E}(V_n + \alpha \delta V_n) &= \mathcal{E}(V_n) + \alpha \left\langle \nabla \mathcal{E}_{|V=V_n} \middle| \delta V_n \right\rangle \\ &\quad + \frac{\alpha^2}{2} \left\langle \delta V_n \middle| \nabla^2 \mathcal{E}_{|V=V_n} \delta V_n \right\rangle + O(\alpha^3 \|\delta V_n\|^3)\end{aligned}$$

- ... and some algebra:

$$\begin{aligned}\nabla \mathcal{E}_{|V=V_n} &= \chi_0(V_n) \left[V(\rho(V_n)) - V_n \right] \\ \nabla^2 \mathcal{E}_{|V=V_n} &= \chi_0(V_n) \left[K(\rho(V_n)) \chi_0(V_n) - 1 \right] \\ &\quad + \chi'_0(V_n) \left[V(\rho(V_n)) - V_n \right]\end{aligned}$$

where

- Hartree-XC kernel $K(\rho) = \nabla_\rho^2 E_{\text{Hxc}}(\rho)$
- Independent-particle susceptibility $\chi_0(V) = \rho'(V)$

Constructing the model (1)

- Use Taylor ...

$$\begin{aligned}\mathcal{E}(V_n + \alpha \delta V_n) &= \mathcal{E}(V_n) + \alpha \left\langle \nabla \mathcal{E}_{|V=V_n} \middle| \delta V_n \right\rangle \\ &\quad + \frac{\alpha^2}{2} \left\langle \delta V_n \middle| \nabla^2 \mathcal{E}_{|V=V_n} \delta V_n \right\rangle + O(\alpha^3 \|\delta V_n\|^3)\end{aligned}$$

- ... and some algebra:

$$\begin{aligned}\nabla \mathcal{E}_{|V=V_n} &= \chi_0(V_n) \left[V(\rho(V_n)) - V_n \right] \\ \nabla^2 \mathcal{E}_{|V=V_n} &= \chi_0(V_n) \left[K(\rho(V_n)) \chi_0(V_n) - 1 \right] \\ &\quad + \underbrace{\chi'_0(V_n)}_{\simeq 0 \text{ near convergence}} \left[V(\rho(V_n)) - V_n \right]\end{aligned}$$

where

- Hartree-XC kernel $K(\rho) = \nabla_\rho^2 E_{\text{Hxc}}(\rho)$
- Independent-particle susceptibility $\chi_0(V) = \rho'(V)$

Constructing the model (1)

- Use Taylor ...

$$\begin{aligned}\mathcal{E}(V_n + \alpha \delta V_n) &= \mathcal{E}(V_n) + \alpha \left\langle \nabla \mathcal{E}_{|V=V_n} \middle| \delta V_n \right\rangle \\ &\quad + \frac{\alpha^2}{2} \left\langle \delta V_n \middle| \nabla^2 \mathcal{E}_{|V=V_n} \delta V_n \right\rangle + O(\alpha^3 \|\delta V_n\|^3)\end{aligned}$$

- ... and some algebra:

$$\nabla \mathcal{E}_{|V=V_n} = \chi_0(V_n) \left[V(\rho(V_n)) - V_n \right]$$

$$\nabla^2 \mathcal{E}_{|V=V_n} \simeq \chi_0(V_n) \left[K(\rho(V_n)) \chi_0(V_n) - 1 \right]$$

where

- Hartree-XC kernel $K(\rho) = \nabla_\rho^2 E_{\text{Hxc}}(\rho)$
- Independent-particle susceptibility $\chi_0(V) = \rho'(V)$

Constructing the model (2)

- Using the self-adjointness of χ_0 this yields:

$$\begin{aligned}\varphi_n(\alpha) &= \mathcal{E}(V_n) + \alpha \langle V(\rho(V_n)) - V_n | \chi_0(V_n) \delta V_n \rangle \\ &\quad + \frac{\alpha^2}{2} \left[\langle \chi_0(V_n) \delta V_n | K(\rho(V_n)) \chi_0(V_n) \delta V_n \rangle \right. \\ &\quad \left. - \langle \delta V_n | \chi_0(V_n) \delta V_n \rangle \right]\end{aligned}$$

- Application of χ_0 is expensive (involves linear system):

$$\alpha \chi_0(V_n) \delta V_n = \rho(V_n + \alpha \delta V_n) - \rho(V_n) + O(\alpha^2 \|\delta V_n\|^2)$$

- Now: Expensive step is $\rho(V)$ (involves diagonalisation)
 - $\rho(V_n)$ known (needed to construct δV_n)
 - $\rho(V_n + \alpha \delta V_n) = \rho(V_{n+1})$ (if accepted) \Rightarrow diagonalisation reuse
- \Rightarrow More efficient than standard line search strategies (e.g. Armijo)

Constructing the model (2)

- Using the self-adjointness of χ_0 this yields:

$$\begin{aligned}\varphi_n(\alpha) &= \mathcal{E}(V_n) + \alpha \langle V(\rho(V_n)) - V_n | \chi_0(V_n) \delta V_n \rangle \\ &\quad + \frac{\alpha^2}{2} \left[\langle \chi_0(V_n) \delta V_n | K(\rho(V_n)) \chi_0(V_n) \delta V_n \rangle \right. \\ &\quad \left. - \langle \delta V_n | \chi_0(V_n) \delta V_n \rangle \right]\end{aligned}$$

- Application of χ_0 is expensive (involves linear system):

$$\alpha \chi_0(V_n) \delta V_n = \rho(V_n + \alpha \delta V_n) - \rho(V_n) + O(\alpha^2 \| \delta V_n \|^2)$$

- Now: Expensive step is $\rho(V)$ (involves diagonalisation)
 - $\rho(V_n)$ known (needed to construct δV_n)
 - $\rho(V_n + \alpha \delta V_n) = \rho(V_{n+1})$ (if accepted) \Rightarrow diagonalisation reuse
- \Rightarrow More efficient than standard line search strategies (e.g. Armijo)

Adaptive damping algorithm

Input: Current iterate V_n , search direction δV_n , trial damping $\tilde{\alpha}$

Output: Damping α_n , next iterate V_{n+1}

```
1: Initialise  $\alpha_n \leftarrow \tilde{\alpha}$ 
2: loop
3:   Make tentative step  $V_{n+1} = V_n + \alpha_n \delta V_n$ 
4:   Compute  $\rho(V_{n+1}), \mathcal{E}(V_{n+1})$  (the expensive step)
5:   if accept  $V_{n+1}$  (details follow) then
6:     break
7:   else
8:     Build the coefficients of the model  $\varphi_n$ 
9:     if model  $\varphi_n$  is good (details follow) then
10:        $\alpha_n \leftarrow \arg \min_{\alpha} \varphi_n(\alpha)$ 
11:       Scale  $\alpha_n$  to ensure  $|\alpha_n|$  is strictly decreasing
12:     else
13:        $\alpha_n \leftarrow \frac{\alpha_n}{2}$ 
14:     end if
15:   end if
16: end loop
```

Notes and details

- Step acceptance: Energy or residual decrease

$$\mathcal{E}(V_{n+1}) < \mathcal{E}(V_n) \quad \text{or} \quad V(\rho(V_{n+1})) - V_{n+1} < V(\rho(V_n)) - V_n$$

- φ_n is approximate \Rightarrow Only use if prediction error

$$\frac{|\mathcal{E}(V_n + \alpha_n \delta V_n) - \varphi_n(\alpha_n)|}{|\mathcal{E}(V_n + \alpha_n \delta V_n) - \mathcal{E}(V_n)|} \quad \text{is small}$$

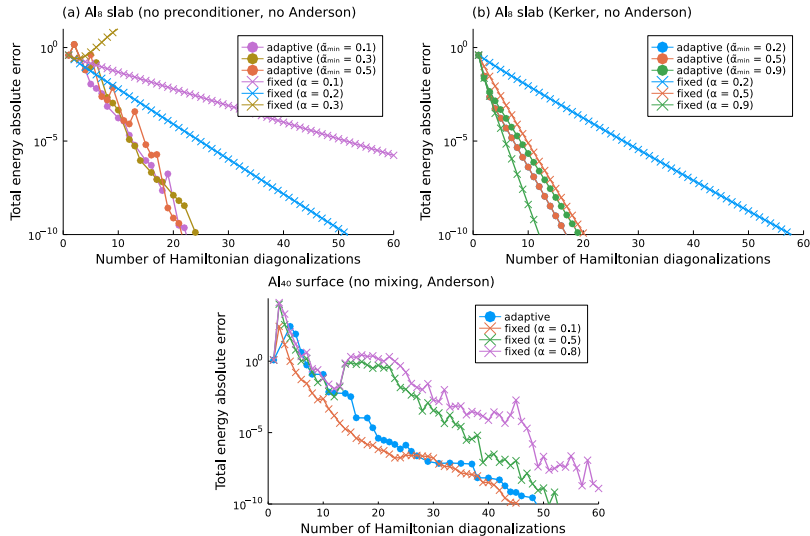
- Adaptive damping costs:

- Only one diagonalisation per line search iteration
- Good trial damping $\tilde{\alpha}$ is crucial

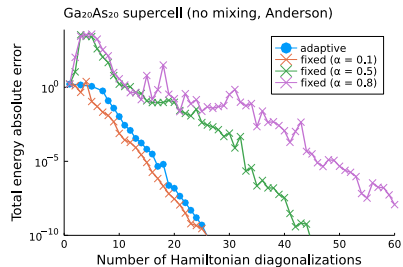
\Rightarrow Dynamical trial damping $\tilde{\alpha}$ adjustment:

- Generally reuse damping from previous SCF step (shrinks α_n)
- If immediately successful ($\alpha_n = \tilde{\alpha}$), use φ_n to grow $\tilde{\alpha}$
- Ensure $\alpha_n \geq \tilde{\alpha}_{\min} = 0.2$ (otherwise stagnation)

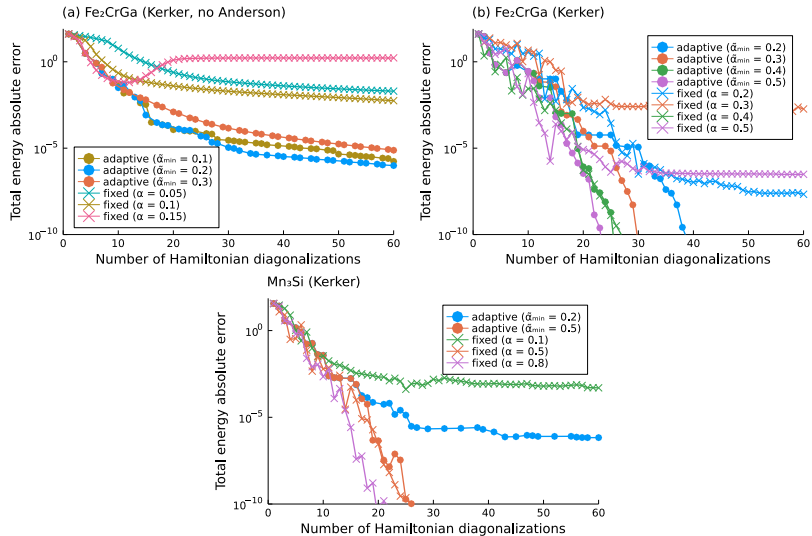
Aluminium slab and surface (simple systems)



GaAs slab (non-linear system)



Fe_2CrGa and Mn_3Si (Heusler systems)



Contents

- 4 LDOS preconditioner
- 5 Adaptive damping
- 6 Algorithmic differentiation
- 7 A posteriori



How does algorithmic differentiation (AD) work?

- $F : \mathbb{R}^2 \rightarrow \mathbb{R}$ with

$$F(x) = \text{double}(\text{sum}(x_1, x_2))$$

```
function F(x)
    y1 = x[1] + x[2] # F1 = sum
    y2 = 2 * p         # F2 = double
    return y2
end
```

- Derivative at \tilde{x} :

$$[J_F(\tilde{x})]_{ij} = \left(\frac{\partial F}{\partial x} \Big|_{x=\tilde{x}} \right)_{ij} = \frac{\partial F_i}{\partial x_j} \Big|_{x=\tilde{x}}$$

- AD: Compose Jacobian of F from known Jacobians of primitives of computational graph:

$$\begin{aligned} e_i^T J_F e_j &= e_i^T (\text{J}_{\text{double}} \text{J}_{\text{sum}} e_j) && \text{"Forward mode"} \\ &= \left(\text{J}_{\text{sum}}^T \text{J}_{\text{double}}^T e_i \right)^T e_j && \text{"Adjoint mode"} \end{aligned}$$

- Devil is in the details:

- E.g. adjoint mode: Reverse control flow ("back propagation")

Forward-mode algorithmic differentiation

```
function F(x)
    y1 = x[1] + x[2] # F1 = sum
    y2 = 2 * p         # F2 = double
    return y2
end
```

$$F(x) = \text{double}(\text{sum}(x_1, x_2))$$

$$e_i^T J_F e_j = e_i^T J_{\text{double}} J_{\text{sum}} e_j$$

- **Forward-diff:** Evaluate in order with *primal* F :

- ① Set $y_0 = (x_1, x_2)$, $\dot{y}_0 = e_j$
- ② Compute $y_1 = \text{sum}(y_0)$ and $\dot{y}_1 = J_{\text{sum}}(y_0)\dot{y}_0$
- ③ Compute $y_2 = \text{double}(y_1)$ and $\dot{y}_2 = J_{\text{double}}(y_1)\dot{y}_1$
- ④ Obtain $F(x_1, x_2)$ as y_2 and $[J_F]_{:,j} = \dot{y}_2$

⇒ Obtain one column of J_F at a time

- Advantage: Numbers → **dual numbers**
- Disadvantage: Gradients require $\mathcal{O}(N)$ times primal cost

Adjoint-mode algorithmic differentiation

```
function F(x)
    y1 = x[1] + x[2] # F1 = sum
    y2 = 2 * p         # F2 = double
    return y2
end
```

$$F(x) = \text{double}(\text{sum}(x_1, x_2))$$

$$e_i^T J_F e_j = \left(J_{\text{sum}}^T J_{\text{double}}^T e_i \right)^T e_j$$

- Adjoint-mode AD: Derivative in reverse instruction order.
- Forward pass:

- ① Set $y_0 = (x_1, x_2)$
- ② Compute $y_1 = \text{sum}(y_0)$ and store it
- ③ Compute $y_2 = \text{double}(y_1)$ and store it

- Reverse pass:

- ① Set $\bar{y}_2 = e_i$
- ② Compute $\bar{y}_1 = [J_{\text{double}}(y_1)]^T \bar{y}_2 \leftarrow$
- ③ Compute $\bar{y}_0 = [J_{\text{sum}}(y_0)]^T \bar{y}_1 \leftarrow$

- Obtain $[J_F]_{i,:}$ as $\bar{y}_0^T \implies$ One row at a time, $\mathcal{O}(1)$ times primal

Properties and derivatives of SCFs

- SCF fixed-point problem in density matrix P

$$0 = f(P, \lambda) = f_{\text{FD}}(H^\lambda(P)) - P$$

with

- λ : Parameters (*for simplicity*: both external & neural net)
- f_{FD} : Fermi-Dirac function
- H^λ : Non-linear Kohn-Sham Hamiltonian
- Defines implicit function $P(\lambda)$ for density matrix
- Quantities of interest:

$$\frac{dA(P)}{d\lambda} = \frac{\partial A}{\partial \lambda} + \frac{\partial A}{\partial P} \frac{\partial P}{\partial \lambda}$$

- Forces: $A = E$, $\lambda = R$ (atomic displacement)
- Polarisability: $A = \text{dipole moment}$, $\lambda = \mathcal{E}$ (electric field)

Response theory (1)

- If $A \neq E$ we need $\frac{\partial P}{\partial \lambda}$
- Consider at $\lambda = \lambda_*$ and corresponding P_* and H_* :

$$\begin{aligned} 0 &= \frac{\partial}{\partial \lambda} \left[f_{\text{FD}}(H^\lambda(P)) - P \right] \Big|_* \\ &= f'_{\text{FD}}(H_*) \cdot \frac{\partial H^\lambda}{\partial \lambda} \Big|_* + \frac{\partial P}{\partial \lambda} \Big|_* \cdot \frac{\partial}{\partial P} \left[f_{\text{FD}}(H^\lambda(P)) - P \right] \Big|_* \\ &= f'_{\text{FD}}(H_*) \cdot \frac{\partial H^\lambda}{\partial \lambda} \Big|_* + \frac{\partial P}{\partial \lambda} \Big|_* \cdot \left[f'_{\text{FD}}(H_*) \cdot K^{\lambda_*}(P_*) - I \right] \\ &= \chi_0(H_*) \cdot \frac{\partial H^\lambda}{\partial \lambda} \Big|_* - \frac{\partial P}{\partial \lambda} \Big|_* \cdot \left[I - \chi_0(H_*) \cdot K^{\lambda_*}(P_*) \right] \end{aligned}$$

where $K^{\lambda_*} = \frac{\partial H^{\lambda_*}}{\partial P}$, $\chi_0(H_*) = f'_{\text{FD}}(H_*)$

Response theory (2): Sternheimer equation

$$0 = \chi_0(H_*) \cdot \frac{\partial H^\lambda}{\partial \lambda} \Big|_* - \frac{\partial P}{\partial \lambda} \Big|_* \cdot [I - \chi_0(H_*) \cdot \mathbf{K}^{\lambda*}(P_*)]$$

- Rearrange:

$$\begin{aligned}\frac{\partial P}{\partial \lambda} \Big|_* &= [I - \chi_0(H_*) \mathbf{K}^{\lambda*}(P_*)]^{-1} \chi_0 \frac{\partial H^\lambda}{\partial \lambda} \Big|_* \\ &= - [\mathbf{K}^{\lambda*}(P_*) + \boldsymbol{\Omega}(H_*)]^{-1} \frac{\partial H^\lambda}{\partial \lambda} \Big|_*\end{aligned}$$

$$\text{where } \boldsymbol{\Omega}(H_*) = -[\chi_0(H_*)]^{-1}$$

- Sternheimer equation (implicit differentiation)

Contents

- 4 LDOS preconditioner
- 5 Adaptive damping
- 6 Algorithmic differentiation
- 7 A posteriori



Applied and
Computational
Mathematics

RWTHAACHEN
UNIVERSITY

Estimating the residual

- P_X : Projector into X basis
- Split up residual into contributions:

$$\|\tilde{r}\| = \|P_X \tilde{r}\| + \|P_{X^\perp} \tilde{r}\| = \|P_X \mathbf{H} \tilde{u} - \tilde{\varepsilon} \tilde{u}\| + \|P_{X^\perp} \mathbf{V} \tilde{u}\|$$

(Use $P_X \tilde{u} = \tilde{u}$ and diagonal kinetic operator)

- $\|P_X \tilde{r}\|$: Residual inside X (**algorithm error**)
- $\|P_{X^\perp} \tilde{r}\|$: Residual outside X (**discretisation error**)

Estimating the residual (2)

- Dual-basis approach:
 - X is discretisation basis (used for main computation)
 - $Y \supset X$: Basis on which V can be computed
- Second split:

$$\|P_{X^\perp} V \tilde{u}\| = \|P_{X^\perp \cap Y} V \tilde{u}\| + \|P_{Y^\perp} V \tilde{u}\|$$

- First term computable, second term is

$$\|P_{Y^\perp} V \tilde{u}\|^2 = \sum_{G \in Y^\perp} \left| \sum_{G' \in X} \langle e_G | V e_{G'} \rangle \tilde{u}(G') \right|^2$$

- By construction: $\hat{v}_{\text{loc}}(G)$ and $p_{Li}(k + G)$ decay outside Y
- ⇒ Elements $\langle e_G | V e_{G'} \rangle$ coupling X and Y^\perp are small!
- ⇒ Can derive upper bound for $\|P_{Y^\perp} V \tilde{u}\|$

Bound on residual (local)

$$\begin{aligned}
& \Omega^2 \|P_{Y^\perp} V_{\text{loc}} \tilde{u}\|^2 \\
&= \sum_{G \in Y^\perp} \left| \sum_{G' \in X} V_{\text{loc}}(G - G') \tilde{u}(G') \right|^2 \quad \text{Next introduce Sobolev weight \& CS in } G' \\
&\leq \left(\sum_{G' \in X} (1 + |G'|^2)^{-s} \right) \sum_{G \in Y^\perp} \sum_{G' \in X} \left| V_{\text{loc}}(G - G') (1 + |G'|^2)^{s/2} \tilde{u}(G') \right|^2 \\
&= \left(\sum_{G' \in X} (1 + |G'|^2)^{-s} \right) \sum_{G' \in X} (1 + |G'|^2)^s |\tilde{u}(G')|^2 \sum_{G \in Y^\perp} \left| V_{\text{loc}}(G - G') \right|^2 \\
&\leq \left(\sum_{G' \in X} (1 + |G'|^2)^{-s} \right) \sum_{G' \in X} (1 + |G'|^2)^s |\tilde{u}(G')|^2 \sum_{\substack{\Delta G \in \mathcal{R}^* \\ |\Delta G| > \sqrt{2E_{\text{cut}}^{(2)}} - |G'|}} |V_{\text{loc}}(\Delta G)|^2 \\
&= \left(\sum_{G' \in X} (1 + |G'|^2)^{-s} \right) \sum_{G' \in X} (1 + |G'|^2)^s |\tilde{u}(G')|^2 S_{\mathcal{R}^*} \left(|V_{\text{loc}}|^2, \sqrt{2E_{\text{cut}}^{(2)}} - |G'| \right)
\end{aligned}$$

- We chose $s = 0$

Bound on opnorm (local)

Used for $\|P_{X^\perp} V_{\text{loc}} P_X\|_{\text{op}}$, $\|P_{Y^\perp} V_{\text{loc}} P_X\|_{\text{op}}$, $\|P_{X^\perp} V_{\text{loc}} P_{X^\perp}\|_{\text{op}}$.

$$\begin{aligned}\|V_{\text{loc}}\|_{\text{op}} &\leq \frac{1}{\Omega} \left(\left\| \sum_{G \in Y} \widehat{v}_{\text{loc}}(G) e^{iG \cdot r} \right\|_\infty + \sum_{G \in Y^\perp} |\widehat{v}_{\text{loc}}| \right) \\ &\leq \frac{1}{\Omega} \left(\left\| \sum_{G \in Y} \widehat{v}_{\text{loc}}(G) e^{iG \cdot r} \right\|_\infty + S_{\mathcal{R}^*}(|\widehat{v}_{\text{loc}}|, \sqrt{2E_{\text{cut}}}) \right),\end{aligned}$$

where $\|v\|_\infty = \sup_{r \in \mathbb{R}^3} |v(r)|$. To bound the first term, we use the fact that for a regular grid \mathfrak{G} of the unit cell, we have

$$\left\| \sum_{G \in Y} \widehat{v}_{\text{loc}}(G) e^{iG \cdot r} \right\|_\infty \leq \max_{r \in \mathfrak{G}} \left| \sum_{G \in Y} \widehat{v}_{\text{loc}}(G) e^{iG \cdot r} \right| + \delta \sum_{G \in Y} |G| |\widehat{v}_{\text{loc}}(G)|$$

where δ is the diameter of the grid.

Bound on the residual (non-local)

- Focus on term only:

$$\langle e_G | v_{\text{nl}} | e_{G'} \rangle = p^{(1)}(k + G) \overline{p^{(2)}(k + G')},$$

- Define

$$c_{\tilde{u}} = \sum_{G \in X} \overline{p^{(2)}(k + G)} \tilde{u}(G)$$

$$\begin{aligned}\|P_{Y^\perp} v_{\text{nl}} \tilde{u}\|^2 &= |c_{\tilde{u}}|^2 \sum_{G \in Y^\perp} |p^{(1)}(k + G)|^2 \\ &\leq |c_{\tilde{u}}|^2 \|Y_{lm}\|_\infty^2 \sum_{G \in Y^\perp} |R^{(1)}(|G| - |k|)|^2 \\ &= |c_{\tilde{u}}|^2 \|Y_{lm}\|_\infty^2 S_{\mathcal{R}^*} \left(|R^{(1)}(\cdot - |k|)|^2, \sqrt{2E_{\text{cut}}^{(2)}} \right),\end{aligned}$$

Bound on opnorm (non-local)

- By Hilbert–Schmidt-operator-norm inequality:

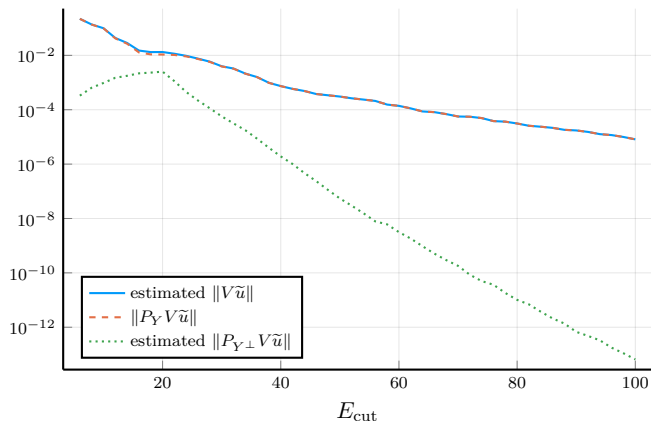
$$\begin{aligned}\|P_{Y^\perp} v_{\text{nI}} P_X\|_{\text{op}} &\leq \|P_{X^\perp} v_{\text{nI}} P_X\|_{\mathfrak{S}_2} \\ &= \sum_{G \in Y^\perp} |p^{(1)}(k + G)|^2 \cdot \sum_{G \in X} |p^{(2)}(k + G)|^2\end{aligned}$$

- Additionally:

$$\begin{aligned}\|P_{X^\perp} v_{\text{nI}} P_{X^\perp}\|_{\text{op}}^2 &\leq \|Y_{lm}\|_\infty^4 \quad S_{\mathcal{R}^*}(|R^{(1)}(\cdot - |k|)|^2, \sqrt{2E_{\text{cut}}}) \\ &\quad S_{\mathcal{R}^*}(|R^{(2)}(\cdot - |k|)|^2, \sqrt{2E_{\text{cut}}}).\end{aligned}$$

Numerical results for residual estimate

- $E_{\text{cut}}^{(2)}$ (and thus Y) fixed empirically to $4E_{\text{cut}}$



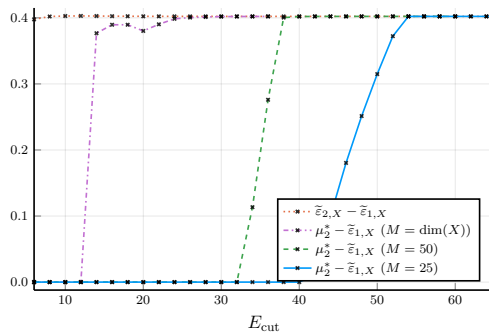
Details on lower bounds on eigenvalue ε_{n+1}

- Strategy to find μ :

- Guess $\mu \in (\tilde{\varepsilon}_n, \tilde{\varepsilon}_{n+1})$
- Use computed bounds to find largest μ such that

$$E_{\text{cut}} + \|V_{X^\perp X^\perp}\|_{\text{op}} - \mu - B_\mu \geq 0$$

\Rightarrow If exists, proves that μ is guaranteed lower bound to δ



Arithmetic error

- Interval arithmetic: Represent $x \in \mathbb{R}$ by interval

$$[a, b] \quad a, b \in \text{DP}, \quad a \leq x \leq b$$

- Can be used as floating-point type in  DFTK
- ⇒ Compute in-basis $\|P_X \tilde{r}\|$: Sum **arithmetic + algorithm** error

